International Journal of Pharmaceutics 381 (2009) 160–165

Contents lists available at ScienceDirect

International Journal of Pharmaceutics

journal homepage: www.elsevier.com/locate/ijpharm

Preparation and characterization of dextran nanobubbles for oxygen delivery

R. Cavalli[a,*], A. Bisazza[a], P. Giustetto[b], A. Civra[c], D. Lembo[c], G. Trotta[a], C. Guiot[b], M. Trotta[a]

[a] Dipartimento di Scienza e Tecnologia del Farmaco, Università degli Studi di Torino - Via Pietro Giuria 9 - 10125, Torino, Italy
[b] Dipartimento di Neuroscienze, Università degli Studi di Torino - Corso Raffaello 30 - 10125, Torino, Italy
[c] Dipartimento di Scienze Cliniche e Biologiche, Università degli Studi di Torino, Ospedale S. Luigi Gonzaga, 10043 Orbassano, Torino, Italy

ARTICLE INFO

Article history:
Received 12 December 2008
Received in revised form 10 March 2009
Accepted 10 July 2009
Available online 17 July 2009

Keywords:
Dextran
Oxygen delivery
Hypoxia
Nanobubbles
Ultrasound

ABSTRACT

Dextran nanobubbles were prepared with a dextran shell and a perfluoropentan core in which oxygen was stored. To increase the stability polyvinylpirrolidone was also added to the formulation as stabilizing agent. Rhodamine B was used as fluorescent marker to obtain fluorescent nanobubbles. The nanobubble formulations showed sizes of about 500 nm, a negative surface charge and a good capacity of loading oxygen, no hemolytic activity or toxic effect on cell lines. The fluorescent labelled nanobubbles could be internalized in Vero cells. Oxygen-filled nanobubbles were able to release oxygen in different hypoxic solutions at different time after their preparation in *in vitro* experiments. The oxygen release kinetics could be enhanced after nanobubble insonation with ultrasound at 2.5 MHz. The oxygen-filled nanobubble formulations might be proposed for therapeutic applications in various diseases.

1. Introduction

Oxygen is one of the key elements in cell metabolism, and its concentration in tissues plays an important role in regulating biochemical reactions (Wagner, 2008, Soleymanlou et al., 2005).

Reduced oxygen supply from the arterial blood to cells substantially increases the risk of inflammation, infection and scarring, reduces the efficacy of medical treatments and may ultimately lead to tissue necrosis. Many medical conditions, such as diabetes, burns, bedsores and wounds are related to insufficient supply of oxygen to the tissues; oxygen deficiency, together with acidosis, is also the main hallmark of cancerous solid tumors and a major factor limiting the effectiveness of radiotherapy (Asimov et al., 2007). These are therefore possible fields of application of oxygen-filled nanobubbles besides other oxygenation approches (Al-Waili et al., 2005, Overgaard, 1994). Another potential field for nanobubbles application is that of anaerobic infections. Anaerobic bacteria grow where oxygen is completely, or almost completely, lacking and they can cause infections when a normal barrier, such as the skin, gums, or intestinal wall, is damaged due to surgery, injury, or disease. The targeted release of oxygen by means of delivery system may be a useful adjuvant to antibiotic therapy of anaerobic infections.

The delivery of oxygen has been examined in various studies (Van Liew and Burkard, 1996, Burkard and Van Liew, 1994) Hemoglobin-loaded particles (Hb-particles) encapsulated within a biodegradable polymer have been prepared for use as oxygen carriers (Zhao et al., 2007). The Hb-particles exhibited oxygen-carrying capacity similar to that of native hemoglobin and showed prolonged circulation time after *in vivo* administration in mice. Dextrose albumin microbubbles for oxygen and nitrogen delivery have been formulated (Porter et al., 1998) for use as contrast agents. Oxygen-enriched lipid-coated perfluorocarbon microbubbles have been prepared for oxygen delivery; these oxygen-enriched microbubbles were tested in a model of anemic rats (Unger et al., 2004; Unger et al., 2002) and maintained the rat's survival at very low hematocrit levels.

Oxygen-filled chitosan microbubbles showed to act as an efficient oxygen delivery system (Cavalli et al., 2009). The *in vitro* oxygen release from the chitosan microbubbles in hypoxic media was previously evaluated before and after ultrasound (US) sonication, and the results supported the hypothesis that US enhances gas delivery. Preliminary investigations on the biological effect of such oxygen release on the cellular activity were also undertaken, and an effect on the expression of Hypoxia Inducible Factor-1α (HIF-1) from hypoxic human choriocarcinoma cells after oxygen-filled microbubble delivery was demonstrated (Bisazza et al., 2008).

The aim of the present study was to develop a new bubble formulation in the nanometer size range for use as an innovative oxygen-delivery system.

New formulations were developed, consisting of nanobubbles with a dextran coating and bubble stabilization was improved, both by adding a poorly soluble gas (perfluoropentan) to the core and (Lundgren et al., 2006) by adding polyvinylpyrrolidone (PVP) to the shell. The resulting nanobubbles were characterized by their sizes, chemical properties, oxygen release efficiency, biocompatibility

* Corresponding author. Tel.: +39 011 6707825; fax: +39 011 6707687.
E-mail address: roberta.cavalli@unito.it (R. Cavalli).

0378-5173/$ – see front matter © 2009 Elsevier B.V. All rights reserved.
doi:10.1016/j.ijpharm.2009.07.010

Table 1
Composition of the three formulations.

Components	Formulation A (%, w/v)	Formulation B (%, w/v)	Formulation C (%, w/v)
Palmitic acid	0.02	0.02	0.01
Epikuron® 200	0.02	0.05	0.05
Perfluoropentan	7.02	6.70	6.58
Filtered water	88.53	88.80	89.06
Dextran	0.17	0.16	0.16
Pvp	–	0.25	–
Ethanol	4.24	4.02	3.98
Deae + rhodamine B	–	–	0.16

and cellular uptake, in view of their possible applications in treating chronic wounds and anaerobic infections.

2. Materials and methods

2.1. Materials

Ethanol 96° was from Carlo Erba (Milan, I). Epikuron® 200 (soya phosphatidylcholine 95%) was a kind gift from Degussa (Hamburg, D). Palmitic acid, perfluoropentan, dextran sulphate sodium salt (M_w = 100,000), polyvinylpyrrolidone (PVP) (M_w = 24,000) were from Fluka (Buchs, CH). Rhodamine B and diethylamino-ethyl-dextran hydrocloride (DEAE) (M_w = 500,000) were from Sigma Aldrich (St. Louis, USA). Ultra-pure water was obtained using a system 1-800 Milli-Q (Millipore, F). Dulbecco's modified Eagle's medium (DMEM), fetal calf serum and antibiotics for cell culture were from Gibco/BRL (Gaithersburg, MD, USA).

2.2. Preparation of oxygen-filled nanobubbles

An ethanol solution containing Epikuron® 200 (1%, w/v) and palmitic acid (0.3%, w/v) was added to perfluoropentan and ultra-pure water under stirring. The solution was saturated with oxygen up to a gas concentration of 35 mg/l. A 2.7% (w/v) dextran solution (M_w dextran = 100,000) was added drop-wise while the mixture was homogenized, using a high-shear homogenizer (Ultraturrax, Germany) for 2 min at 13,000 rpm and continuing the oxygen purge, in the presence (formulation B) or absence (formulation A) of 5% (w/v) polyvinylpyrrolidone (PVP) solution as stabilizing agent.

Rhodamine B was used as fluorescent marker to prepare fluorescent labelled nanobubbles (Visser et al., 1999). For whose preparation procedure was similar to the above described for formulation A. Rhodamine B (0.002%, w/v) was added drop-wise during the homogeneization step to a 2.7% (w/v) diethylamino-ethyl-dextran hydrocloride (DEAE) solution. Finally a 2.7% (w/v) dextran solution was added drop-wise under stirring. The composition of the nanobubbles is reported in Table 1.

2.3. Characterization of the nanobubble formulations

2.3.1. Size, particle size distribution and zeta potential determination

The average diameters and polydispersity indices of the nanobubble formulations were determined by photocorrelation spectroscopy (PCS) using a 90 Plus instrument (Brookhaven, NY, USA) at a fixed angle of 90° and a temperature of 25 °C. Each value reported is the average of 10 measurements of 3 different formulations. The polydispersity index indicates the size distribution within a nanobubble population. The electrophoretic mobility and zeta potential of the formulations were determined using a 90 Plus instrument (Brookhaven, NY, USA). For zeta potential determination, samples of the formulation were placed in the electrophoretic cell, where an electric field of about 15 V/cm was applied. Each sample was analyzed at least in triplicate. The electrophoretic mobility measured was converted into zeta potential using the Smoluchowsky equation (Sze et al., 2003).

2.3.2. Morphological analysis

The morphology of nanobubble formulations was determined by Transmission Electron Microscopy (TEM). TEM analysis was carried out using a Philips CM10 instrument (Eindoven, NL). The nanobubble preparations were dropped onto a Formwar-coated copper grid and air-dried before observation. The morphology of fluorescent nanobubbles was determined by fluorescent microscopy employing a Leitz (Germany) instrument.

2.3.3. Stability of the formulations

To determine the stability of formulations A and B upon dilution, the nanobubble fomulations were diluted 1:10 (v/v) with saline solution (0.9% NaCl) and with rat plasma solution (plasma:phosphate buffer pH 7.4, 1:4, v/v) at 25 and 37 °C. After 5, 10, 15 min, 1 and 24 h of incubation their size, size distribution and zeta potential values were measured by photocorrelation spectroscopy (PCS) using a 90 Plus instrument (Brookhaven, NY, USA) at a fixed angle of 90°.

The formulation stability stored at 25 °C was evaluated over time, up to 24 h, determining the oxygen release rate, the morphology and the sizes of nanobubbles by TEM and by PCS, respectively.

2.4. Biocompatibility assessment

2.4.1. Determination of hemolytic activity

The hemolytic activity of formulations A and B was evaluated on human blood. Different percentages (v/v) (1.5%, 2.9%, 5.6%, 8.1%, 9.8%) of nanobubble formulations were added to a suspension of erythrocytes (30%, v/v) in phosphate buffer pH 7.4. A solution containing only a suspension (30%, v/v) of erythrocytes in phosphate buffer pH 7.4 was used as blank. A blank containing an excess of ammonium chloride was used to obtain complete hemolysis as hemolytic control.

After 90 min of incubation at 37 °C the samples were centrifuged at 2000 rpm for 10 min and the supernatant was analyzed using a Lambda 2 Perkin-Elmer spectrophotometer at a wavelength of 543 nm. The percentage of hemolysis was calculated versus the 100% hemolysis control.

2.4.2. Cell viability assay

To test the effect of formulations A and B on cell viability, African green monkey fibroblastoid kidney cells (Vero) were seeded at a density of 1×10^4/well in 96-well plates in DMEM supplemented with 10% of heat-inactivated fetal calf serum and antibiotics.

After 24 h they were incubated with 5 and 10 mg of nanobubbles obtained by appropriate dilutions of the formulations or left untreated. After 48 h cell viability was determined by the CellTiter 96 Proliferation Assay Kit (Promega, Madison, WI, USA) according to the manufacturer's instructions. The effect on cell viability of each formulation at different concentrations was expressed as a percentage, by comparing treated cells with cells incubated with culture medium alone. For the assay, the experiments were performed in triplicate.

2.5. In vitro determination of oxygen release

The oxygen concentration of two 0.9% NaCl (saline) solutions, sealed into two vials, was reduced respectively to 0.4 mg/l (severe hypoxia) and to 4 mg/l (moderate hypoxia) with a N_2 purge, in order to mimic hypoxic conditions. A series of experiments was carried out 5, 30, 60, 180 min and 24 h after the preparation of the formulations to investigate the oxygen release kinetics over time. Then 3 ml

Table 2
Physico-chemical characteristics of the three formulations.

Formulation	Average diameter ± S.D. (nm)	Polydispersity index	PZ ± S.D. (mV)	pH
Formulation A	550 ± 30	0.20	−41 ± 1	6.40
Formulation B	410 ± 5	0.18	−23 ± 2	6.30
Formulation C	520 ± 10	0.25	−37 ± 1	7.40

of oxygen-filled nanobubbles were introduced into 20 ml of each saline solution, and the oxygen release kinetic was monitored for 10 min using an oxymeter (Portamess 913 OXY, Knick). Before each experiment the oxymeter was calibrated in air, after waiting for stable temperature and humidity conditions to be re-established.

2.6. *In vitro determination of oxygen release in the presence of ultrasound*

To study the effect of ultrasound (US) on oxygen release from nanobubbles, a US probe with an oscillation frequency of 2.5 ± 0.1 MHz and an average acoustic pression distribution value of 2.4 ± 0.2 MPa (nominal frequency: 50 Hz; and nominal power: 30 W) was used, combined with a peculiar apparatus consisting of two compartments separated by a silicon membrane. 70 ml of saline solution and 10 ml of oxygen-filled nanobubbles were placed in the first compartment; 20 ml of saline hypoxic solution (0.4 mg/l) were placed in the second compartment. The concentration of oxygen in the hypoxic compartment was monitored for 10 min in the presence of US after 30 min from nanobubbles preparation. To monitor the oxygen concentration, the transducer of the device was held in a fixed position, within the donor compartment. All the experiments were performed in triplicate.

2.7. *Evaluation of cellular uptake through confocal laser scanning microscopy*

African green monkey fibroblastoid kidney cells (Vero) were grown as monolayers in DMEM supplemented with 10% of heat-inactivated fetal calf serum and antibiotics.

Exponentially growing Vero cells were plated and cultured overnight in 24-well plates on glass coverslips; the cell monolayers were incubated with appropriated dilutions of rhodamine-labeled nanobubbles for 1 h and then extensively washed with PBS for observation of live cells. Confocal sections were taken on an inverted Zeiss LSM510 fluorescence microscope.

3. Results

The average diameter, polydispersity index, zeta potential values of oxygen-filled nanobubbles, plus the pH values of their aqueous suspensions, are reported in Table 2.

The sizes of the three nanobubble formulations were below 1 μm, with a rather uniform size distribution. The presence of the fluorescent marker did not affect the diameter of nanobubbles while the presence of PVP formed smaller nanobubbles with a lower polydispersity index. PVP acts as stabilizer agent on the nanobubble surface forming a hydrophylic coating which might impart "stealth-like" properties in view of *in vivo* administration.

The surface of the nanobubbles showed a negative charge that was sufficiently high to prevent nanobubble aggregation. The addition of PVP in the nanobubble formulation decreased the zeta potential and thus confirmed the presence of PVP on the nanobubble surface. TEM analyses showed the spherical shape of nanobubbles confirming their sizes. The TEM image of oxygen-filled formulation A is reported in Fig. 1. The photomicrographs evidenced a clearly visible dextran shell of about 30 nm.

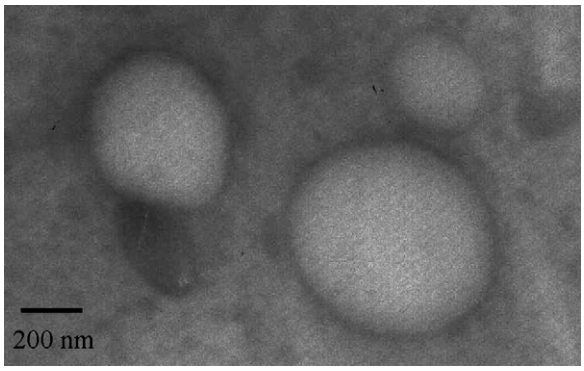

Fig. 1. TEM image of nanobubble formulation A (magnification 27,500×).

The oxygen-filled nanobubbles proved to be stable after dilution both in saline solution and in plasma, after incubation at 25 and 37 °C, as evidenced by TEM and photocorrelation spectroscopy analyses. As shown in Fig. 2A nanobubble average diameters did not change upon dilution in plasma at 25 °C and the stability of the two formulations in the absence or in the presence of PVP is similar over time. At 37 °C PVP increased the nanobubble stability, indeed the diameters of formulation B are maintained over time (Fig. 2B).

The structure stability at 25 °C was confirmed by TEM, 24 h after the nanobubble preparation. The analyses showed that the spherical shape and sizes of the nanobubble formulations did not change 24 h after their preparation (data not shown).

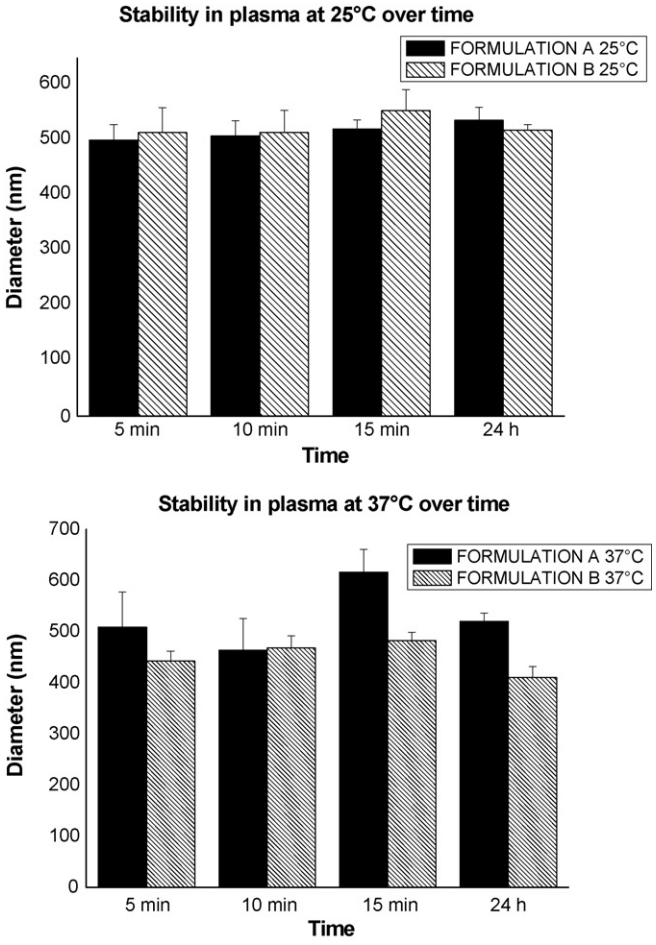

Fig. 2. Stability upon dilution of oxygen-filled nanobubbles over time: (A) in plasma at 25 °C; (B) in plasma at 37 °C.

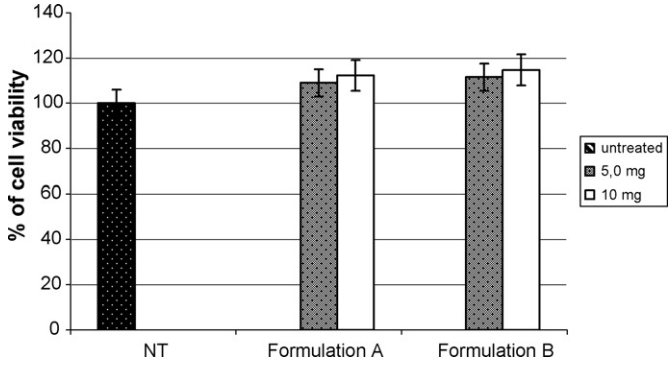

Fig. 3. Effect of formulations A and B on viability of Vero cells as a function of the concentration at 48 h post-treatment. Each point represents the mean ± S.D. ($n = 3$).

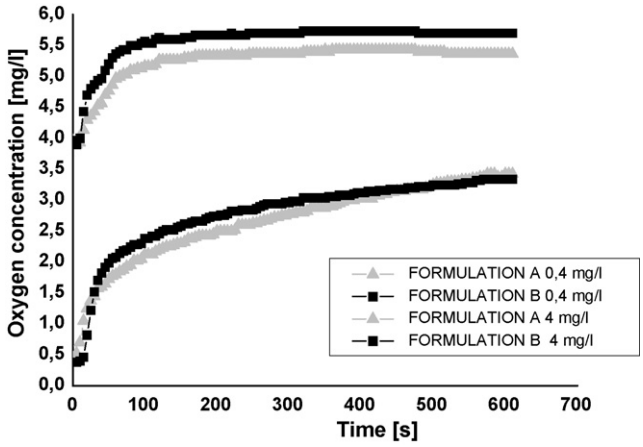

Fig. 4. Oxygen concentration in severe (0.4 mg/l) and moderate (4 mg/l) hypoxic condition after the injection of nanobubble formulation 5 min after their preparation.

Formulations A and B showed no toxicity toward Vero cells after 48 h of incubation at each concentration tested (5 and 10 mg) as shown in Fig. 3.

Moreover the three nanobubble formulations demonstrated no hemolytic activity tested on *in vitro* red blood cells after 90 min incubation at 37 °C.

The oxygen concentration of the two types of hypoxic solutions increased markedly over time after the injection of the oxygen-filled nanobubbles. The nanobubbles showed the capacity of oxygen release either immediately after their preparation either over time. The oxygen increase produced by nanobubbles 5 min after their preparation is reported in Fig. 4. A greater amount of oxygen was released in severe hypoxic conditions (0.4 mg/l) than in moderate hypoxic conditions; producing an increase in the oxygen concentration of about 8-fold after 10 min.

The oxygen release kinetics obtained 30 min, 1 h and 3 h after the preparation of the formulations are reported in Fig. 5. The oxygen release profiles did not change up to 3 h after preparation showing

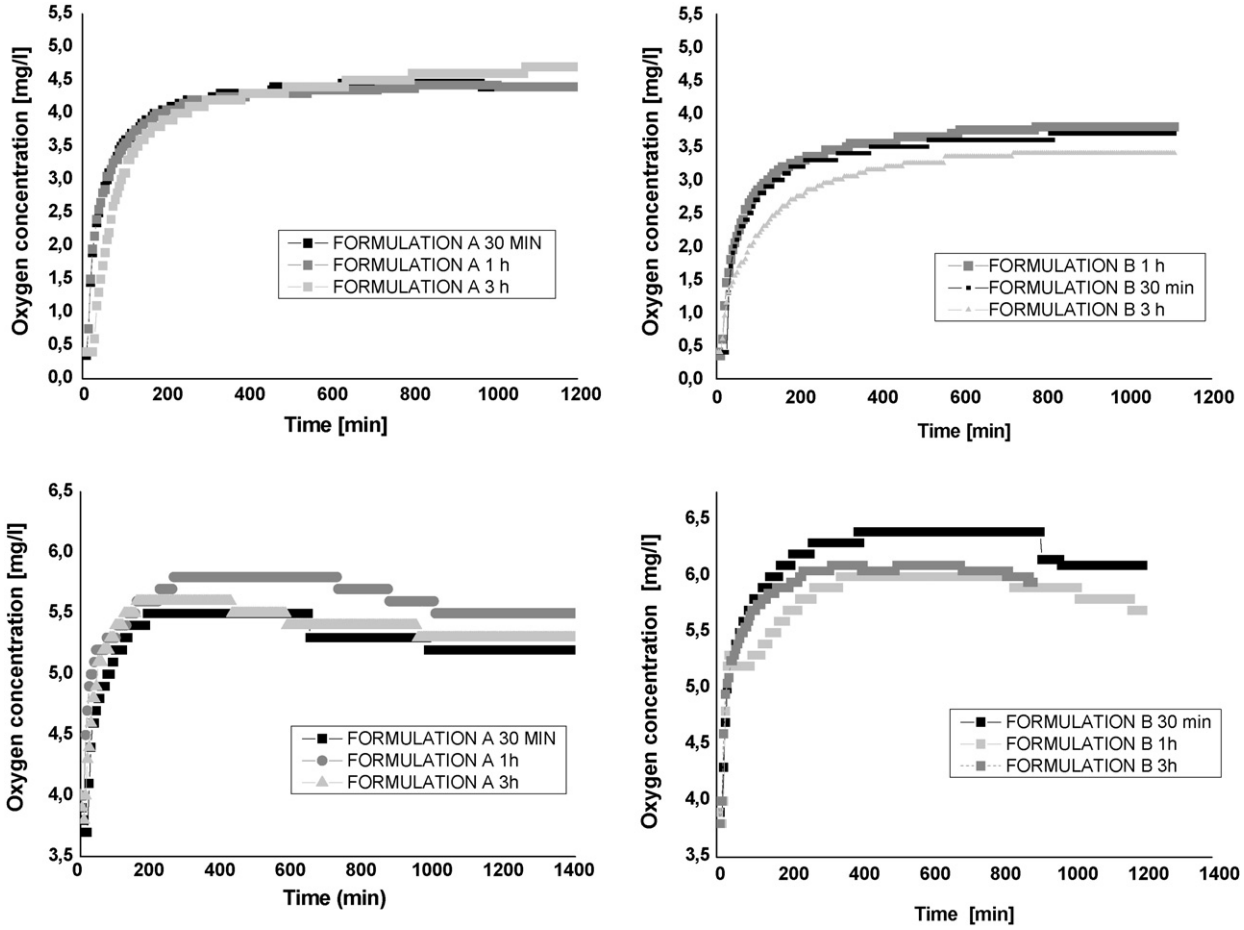

Fig. 5. Oxygen concentration after the injection of nanobubble formulation 30 min, 1 h and 3 h after their preparation. (A) Formulation A severe hypoxia (0.4 mg/l), (B) formulation B severe hypoxia (0.4 mg/l), (C) formulation A moderate hypoxia (4 mg/l), and (D) formulation B moderate hypoxia (4 mg/l).

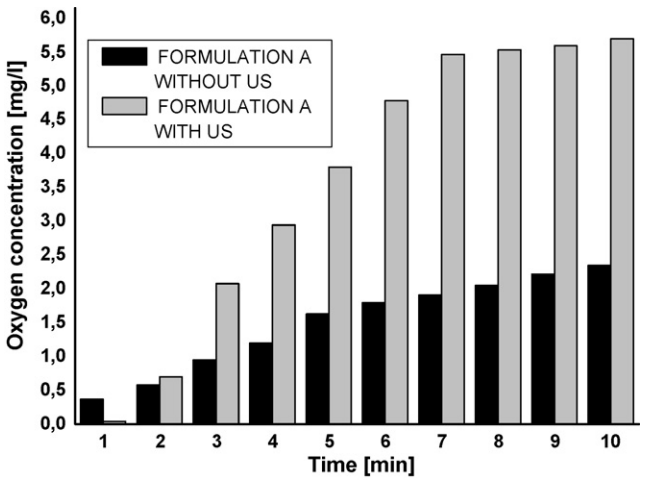

Fig. 6. Oxygen delivery from nanobubble formulation A through a silicon membrane in the presence and absence of US.

the stability of the formulations. Starting from severe hypoxic conditions, the oxygen release kinetics are slower in the presence of the PVP probably due to the greater thickness of the shell. Indeed the oxygen concentration reached about 3.7 mg/l in 2 min for formulation A and the same value in 15 min for PVP-stabilized formulation B. A slower oxygen release kinetics in the presence of PVP were also observed after 24 h from the nanobubble preparation.

US favored oxygen delivery from the oxygen-filled nanobubbles and the release kinetics were faster than those in the absence of US. Fig. 6 shows the oxygen delivery from formulation A nanobubbles through a silicon membrane in the presence of US. The oxygen concentration in the receiving compartment was "incremented" by as much as 133% in the presence of US. A similar kinetic behaviour was obtained with the PVP stabilized nanobubble formulation.

The cellular uptake of fluorescent-labeled nanobubbles was monitored through confocal laser scanning microscopy, on living unfixed cells to avoid artifactual results due to cell fixation protocols. The results demonstrate that after 1 h the nanobubbles are internalized in the cells, and show a diffuse cytoplasmic distribution (Fig. 7) without cytotoxic effects.

This result indicates that nanobubbles might be capable of delivering a gas or a drug directly inside the cells.

4. Discussion

In this study oxygen-filled nanobubbles were prepared using perfluoropentan as core and dextran sulphate, a polysaccharide polymer, as shell. The biocompatibility of dextran-based formulations have been extensively studied (Bos et al., 2005; De Groot et al., 2001). Recently dextran-based hydrogels have been studied as matrices in tissue engineering; no sign of inflammation was detected in *in vivo* experiments (Möller et al., 2007).

The two types of nanobubble formulations as well as the fluorescent one, showed an average diameters lower than 1 μm, a spherical morphology with a core

-shell structure and a negative charge high enough to avoid nanobubble aggregation; consequently they could maintain their structure and small dimension over time. The nanobubble sizes and stability are important properties in view of their potential *in vivo* administration. PVP was added to the formulation to increase nanobubble stability. The choice of PVP was due to its long-standing and safety in biomedical/pharmaceutical applications. PVP is an excipient reported in USP 28 and in other Pharmacopeia as suspending, stabilizing or viscosity-increasing agent admitted for parenteral formulations. PVP solutions may also be used as coating agent. The PVP-stabilized nanobubbles (formulation B) maintained their sizes after dilution with plasma and after incubation at 37 °C. Moreover the size of PVP nanobubbles did not increase over time showing their greater physical stability than formulation A.

The nanobubble structure of the two formulations upon dilution is maintained and it is stable up to 24 h. In heterogeneous systems, it can sometimes happen the formation of a small flocculate after dilution, that could give a precipitate over time. This effect should be favoured by the enhancement of temperature that increase the particle kinetics and the convective movements of particles. The presence of PVP as stabilizing agent could avoid this precipitation phenomena. Moreover, the addition of PVP to the formulation did not affect cell viability.

The nanobubbles prepared had a good oxygen-loading capacity due to the presence of gas core. Perfluoropentan gas can favor oxygen entrapment. On a volume basis, Van Liew has previously shown that gaseous perfluorocarbon compounds may deliver more oxygen than liquid perfluorocarbons (Van Liew and Burkard, 1997). The dextran nanobubbles were able to release oxygen in hypoxic condition. Oxygen could diffuse into the external water phase quickly when the nanobubble formulations are brought into contact with a hypoxic medium. The oxygen was released in greater

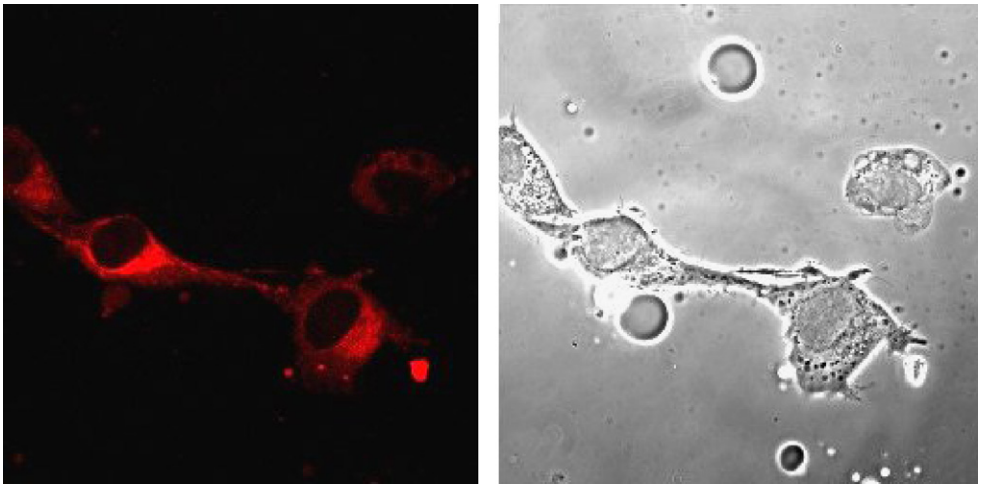

Fig. 7. Cellular uptake of oxygen-filled nanobubbles. Vero cells were incubated for 1 h with the rhodamine-labeled nanobubbles (50 μl) and then analyzed by confocal laser scanning microscopy without fixation. The figure shows phase-contrast (right panel) and immunofluorescence (left panel) images of the same microscopic field. The nanobubbles are internalized with diffuse cytoplasmic distribution.

extent in severe hypoxic condition (oxygen concentration 0.4 mg/l) than in moderate hypoxic condition (oxygen concentration 4 mg/l). A slower release profile was observed in the presence of PVP in hypoxic condition. Ultrasound (US) technology in medicine has developed rapidly over the last decades particularly it's use in diagnostic imaging (Sboros, 2008, Pitt, 2003, Giustetto et al., 2008, Rapoport et al., 2004, Tran et al., 2007).

Nanobubbles can also be cavitated by US energy to increase oxygen release kinetics, which might be useful for possible local site-specific delivery. Ultrasound did not change physical properties of nanobubbles after 10 min of insonation. Hemolitic activity and cell studies showed the biocompatibility of the nanobubble formulations and their capacity to be internalized in the cell without producing toxic effects.

Dextran nanobubbles might be proposed for the delivery of oxygen, and thus might represent a new class of therapeutic systems for various diseases. Particularly the targeted delivery of oxygen by means of US and microbubbles and US may be exploited as an adjuvant to antibiotics whenever anaerobic infection is suspected.

Acknowledgements

The authors would like to thank PRIN 2006 Italian Ministry of University and Ricerca Sanitaria Finalizzata 2006 and 2008 Projects of Regione Piemonte for their support.

References

Al-Waili, N., Butler, G., Beale, J., Hamilton, R., Lee, B., Lucas, P., 2005. Hyperbaric oxygen and malignancies: a potential role in radiotherapy, chemotherapy, tumor surgery and phototherapy. Med. Sci. Monit. 11, RA279–289.

Asimov, M.M., Korolevich, A.N., Kostantinova, E.É., 2007. Kinetics of oxygenation of skin tissue exposed to low-intensity laser radiation. J. Appl. Spectrosc. 74, 133–139.

Bisazza, A., Giustetto, P., Rolfo, A., Caniggia, I., Balbis, S., Guiot, C., Cavalli, R., 2008. Microbubble-mediated oxygen delivery to hypoxic tissues as a new therapeutic device. Conf. Proc. IEEE Eng. Med. Biol. Soc. 2008, 2067–2070.

Bos, G.W., Hennink, W.E., Brouwer, L.A., Wim den Otter, Veldhius, F.J., Van Nostrum, C.F., Van Luyn, M.J.A., 2005. Tissue reactions of in situ formed dextran hydrogels crosslinked by stereocomplex formation after subcutaneous implantation in rats. Biomaterials 26, 3901–3909.

Burkard, M.E., Van Liew, H.D., 1994. Oxygen transport to tissue by persistent bubbles: theory and simulations. J. Appl. Physiol. 77, 2874–2878.

Cavalli, R., Bisazza, A., Rolfo, A., Balbis, S., Madonnaripa, D., Caniggia, I., Guiot, C., 2009. Ultrasound-mediated oxygen delivery from chitosan nanobubbles. Int. J. Pharm. 378, 215–217.

De Groot, C.J., Van Luyn, M.J.A., Van DijK-Wolthuis, Cadée, J.A., Plantinga, J.A., Den Otter, W., Hennink, W.E., 2001. In vitro biocompatibility of biodegradable dextran-based hydrogels tested with human fibroblast. Biomaterials 22, 1197–1203.

Giustetto, P., Bisazza, A., Biagioni, A., Alippi, A., Bettucci, A., Cavalli, R., Guiot, C., 2008. Heat enhances gas delivery and acoustic attenuation in CO_2 filled microbubbles. Conf. Proc. IEEE Eng. Med. Biol. Soc. 2008, 2306–2309.

Lundgren, E.G., Bergoe, G.W., Tyssebotn, I.M., 2006. Intravscular fluorocarbon-stabilized microbubbles protect against fatal anemia in rats. Artif. Cell Blood Subst. Biotechnol. 34, 473–486.

Möller, S., Weisser, J., Bischoff, S., Schnabelrauch, M., 2007. Dextran and hyaluronan methacrilate based hydrogels as matrices for soft tissue reconstruction. Biomol. Eng. 24, 496–504.

Overgaard, J., 1994. Clinical evaluation of nitroimidazoles as modifiers of hypoxia in solid tumors. J. Oncol. Res. 6, 509–518.

Pitt, W.G., 2003. Defining the role of ultrasound in drug delivery. Am. J. Drug Deliv. 1, 27–42.

Porter, T., Kricsfeld, D., Cheathman, S., Li, S., 1998. Effect of blood and microbubble oxygen and nitrogen content on perfluorocarbon-filled dextrose albumin microbubble size and efficacy: in vitro and in vivo studies. J. Am. Soc. Echocardiogr. 11 (5), 421–425.

Rapoport, N.Y., Christensen, D.A., Fain, H.D., Barrows, L., Gao, Z., 2004. Ultrasound triggered drug targeting of tumors in vitro and in vivo. Ultrasonics 42, 943–950.

Sboros, V., 2008. Response of contrast agents to ultrasound. Adv. Drug Del. Rev. 60, 1117–1136.

Soleymanlou, N., Jurisica, I., Nevo, O., Ietta, F., Zhang, X., Zamudio, S., Post, M., Caniggia, I., 2005. Molecular evidence of placental hypoxia inpreeclampsia. J. Clin. Endocrinol. Metab. 90, 4299–4308.

Sze, A., Erickson, D., Ren, L., Li, D., 2003. Zeta-potential measurement using the Smoluchowski equation and the slope of the current–time relationship in electroosmotic flow. J. Colloid Interface Sci. 261, 402–410.

Tran, T.A., Roger, S., Le Guennec, J.Y., Tranquart, F., Bouakaz, A., 2007. Effect of ultrasound on the cell electrophysiological properties. Ultrasound Med. Biol. 33, 158–163.

Unger, E.C., Matsunaga, T.O., McCreery, T., Schumann, P., Sweitzer, R., Quigley, R., 2002. Therapeutic applications of microbubbles. Eur. J. Radiol. 42, 160–168.

Unger, E.C., Porter, T., Culp, W., Labell, R., Matsunaga, T., Zutshi, R., 2004. Therapeutic applications of lipid-coated microbubbles. Adv. Drug Del. Rev. 56, 1291–1314.

Van Liew, H.D., Burkard, M.E., 1997. High oxygen partial pressure in tissue delivered by stabilized microbubbles: theory. Adv. Exp. Med. Biol. 411, 395–401.

Van Liew, H.D., Burkard, M.E., 1996. Relationship of oxygen content to PO_2 for stabilized bubbles in the circulation: theory. J. Appl. Physiol. 81, 500–508.

Visser, N.V., Hink, M.A., Van Hoek, A., Visser, J.W.G., 1999. Comparison between fluorescence correlation spectroscopy and time-resolved fluorescence anisotropy as illustrated with a fluorescent dextran conjugate. J. Fluoresc. 9, 251–255.

Wagner, P.D., 2008. The biology of oxygen. Eur. Resp. J. 31, 887–890.

Zhao, J., Liu, C., Tao, X., Shan, X., Sheng, Y., Wu, F., 2007. Preparation of haemoglobin-loaded nano-sized particles with porous structure as oxygen carriers. Biomaterials 28, 1414–1422.